CONPOINT BETA VERSION: USER'S MANUAL

A CAVITY EXPANSION ANALYSIS PROGRAM FOR THE DETERMINATION OF CONE PENETRATION RESISTANCE AND CAVITY LIMIT PRESSURE

1. Introduction

CONPOINT is a copyrighted FORTRAN code, currently available in its initial version, which does not have modern user interface facilities. The program in its current version calculates either cylindrical or spherical cavity pressure versus strain in sands, given the values of a number of soil variables (for either the Bolton or State Parameter models) and soil state variables (relative density and stress state). It can also be used to compute cone tip resistance if the Bolton model is used together with cylindrical cavity expansion. The program also provides detailed information on the evolution of soil state within the plastic zone around the expanding cavity.

CONPOINT resulted from extensive research done on cone resistance in sands. The program is intended at this time for use in research, although ongoing application of the program to geotechnical practice have been demonstrating its usefulness.

2. Background

CONPOINT is based on the cavity expansion and cone resistance analysis described in detail in Salgado et al. (1997), Salgado and Randolph (2001) and Salgado and Mitchell (2002). By and large, the theory as presented in Salgado et al. (1997) has been superseded by extensions made in the latter two publications, particularly the cone resistance vs. limit pressure relationship, which now accounts for the interface friction angle between the cone and the soil and has a more robust version of the stress rotation analysis presented in Salgado et al. (1997).

3. Cavity Expansion Analysis

The Two Classes of Cavity Expansion Problems

There are two classes of cavity expansion problems: the general problem of cavity expansion from a finite initial radius and the particular case of the creation (and subsequent expansion) of a cavity within a soil mass. The cavity to be expanded or created can be either spherical or cylindrical. Use of the number k = 1 (for cylindrical cavity expansion) and k = 2 (for spherical cavity expansion) allows use of generic equations for both types of cavity. In the realm of soil mechanics, cavity expansion problems have been of great interest to those interested in interpreting the pressuremeter test (e.g., Fahey 1986, Manassero 1989, Palmer 1972, Yu 1994), while cavity creation problems have been used to estimate pile bearing capacity and penetrometer tip resistances (e.g., Bigoni and Laudiero 1989, Carter et al. 1979, Davis et al. 1984, Randolph and Wroth 1979, Randolph et al. 1979, Salgado et al. 1997a, 1997b, 1998, Vesic 1972, 1977). The present analysis can be used for both cavity creation and cavity expansion problems.

Cavity Expansion Analysis by Discretization of Plastic Zone

The one-dimensional nature of the cavity expansion problem is such that elements at different radii all pass successively through the same stress-strain state. Conversely, the pressure-expansion response may be recovered from the conditions at progressively decreasing radii around an expanding cavity. This is illustrated in Figure 1, which provides the basis of the method of analysis described in this paper. The analysis is couched in terms of current (updated) radii r with a typical thin shell bound by inner and outer radii r_i and r_j measured from the center of the cavity, of current radius a. In all cavity expansion/creation problems, combination of the yield criterion

$$\sigma_r = N_{ij}\, \sigma_\theta \qquad (1)$$

for cohesionless soils, with the equilibrium equation

$$\frac{d\sigma_r}{dr} + k\frac{\sigma_r - \sigma_\theta}{r} = 0 \qquad (2)$$

yields

$$\sigma_{r_i} = \sigma_{r_j}\left(\frac{r_j}{r_i}\right)^{k\frac{N_{ij}-1}{N_{ij}}} \qquad (3)$$

where σ_r = radial normal stress around the expanding cavity; N_{ij} = flow number, given by

$$N_{ij} = \frac{1+\sin\phi_{ij}}{1-\sin\phi_{ij}} \qquad (4)$$

and ϕ_{ij} = friction angle within the very thin shell ij. The friction angle, in this paper, is assumed to vary according to one of two models: the state parameter model (Been and Jefferies 1985) or the Bolton model (Bolton 1986). According to the state parameter model,

$$\phi_{ij} - \phi_c = A\,[\exp(-\xi_{ij}) - 1] \qquad (5)$$

where ϕ_c = critical-state friction angle; A = empirical constant that depends on the characteristics of the sand and the type of loading (so that A will not generally be the same for cylindrical and spherical cavity expansion); and ξ_{ij} = state parameter within the thin ij shell, given by

$$\xi_{ij} = v_{ij} + \lambda \ln(p_{ij} / p_A) - \Gamma_A \qquad (6)$$

where v_{ij}, p_{ij} = specific volume (= 1 + void ratio) and mean effective stress within the thin shell ij, respectively; λ, Γ_A = slope and "intercept" (at $p = p_A$) of critical state line in

v-ln p space; p_A = reference stress = 100 kPa = 0.1 MPa (or equivalent value in other units).

According to the Bolton (1986) model,

$$\phi_{ij} = \phi_c + D_\psi \left\{ I_{D,ij} \left[Q + \ln\left(\frac{p_A}{100\, p_{ij}} \right) \right] - R_Q \right\} \tag{7}$$

where D_ψ = 3 for triaxial compression tests and 5 for plane-strain tests; $I_{D,ij}$ = relative density as a number between 0 and 1 within the thin ij shell; Q, R_Q = fitting parameters that depend on the sand characteristics.

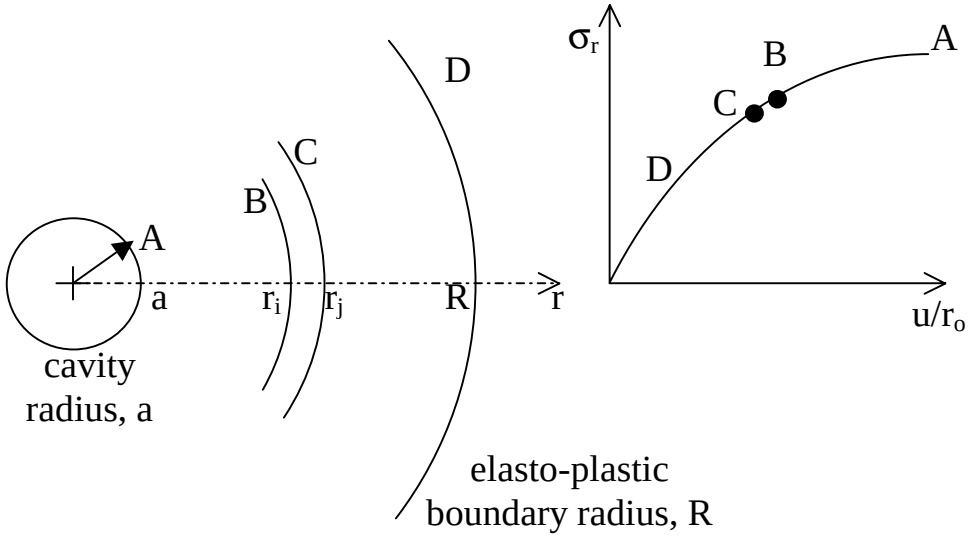

Figure 1 Stress and displacement experienced at two points distant r_i and r_j from cavity center.

In both models, the relationship

$$\phi = \phi_C + 0.8\, \psi \tag{8}$$

proposed by Bolton (1986) between friction and dilatancy angle is assumed to hold.

The radial and hoop strains and the volumetric strain are defined as natural strains in order to accommodate the large deformations near the cavity. For cylindrical cavity expansion, plane strain conditions are in place and $\varepsilon_z = 0$. For spherical cavity expansion, the two tangential normal strains are numerically identical because of symmetry. Thus, for the thin shell element ij, we can write:

$$\varepsilon_r = -\ln\left(\frac{dr}{dr_0}\right) = -\ln\left(\frac{r_j - r_i}{(r_j - u_j) - (r_i - u_i)}\right) \tag{9}$$

$$\varepsilon_\theta = \varepsilon_\varphi = -\ln\left(\frac{r_i}{r_i - u_i}\right) \tag{10}$$

$$\varepsilon_v = -\ln\left(\frac{V}{V_0}\right) = -\ln\left(\frac{r_j^{k+1} - r_i^{k+1}}{(r_j - u_j)^{k+1} - (r_i - u_i)^{k+1}}\right) \tag{11}$$

where u_i and u_j are the deformations associated with radii r_i and r_j, so that that $r_i - u_i$ represents the original, undeformed, radius of the outer boundary of the i^{th} shell).

The plastic strain increments must satisfy the Rowe (1962) flow rule:

$$\sin\psi_{12} = -\frac{\varepsilon_v^{(2)} - \varepsilon_v^{(1)}}{(\varepsilon_r^{(2)} - \varepsilon_r^{(1)}) - k(\varepsilon_\theta^{(2)} - \varepsilon_\theta^{(1)})} \tag{12}$$

where the superscripts (1) and (2), for a given element (i.e., a given value of r), refer to two values of plastic radius $R^{(2)} > R^{(1)}$. Another way to look at this is to consider the indices (1) and (2) to be associated with two adjacent elements i and j, (2) being closer to the cavity than (1), for a given value of plastic radius. This permits rewriting (12) as

$$\sin\psi_{ij} = -\frac{\varepsilon_v^{(i)} - \varepsilon_v^{(j)}}{(\varepsilon_r^{(i)} - \varepsilon_r^{(j)}) - k(\varepsilon_\theta^{(i)} - \varepsilon_\theta^{(j)})} \tag{13}$$

Assuming the radial, hoop and volumetric strains are all known for element j and substituting (9), (10) and (11) into (13) leads to the following equation:

$$\varepsilon_v^{(j)} + \sin\psi_{ij}(\varepsilon_r^{(j)} - k\varepsilon_\theta^{(j)}) = \ln\left(\frac{F_1(u_i)F_2(u_i)}{F_3(u_i)}\right) \tag{14}$$

where

$$F_1(u_i) = \frac{(r_j - u_j)^{k+1} - (r_i - u_i)^{k+1}}{r_j^{k+1} - r_i^{k+1}} \tag{15}$$

$$F_2(u_i) = \left(1 + \frac{u_i - u_j}{r_j - r_i}\right)^{\sin\psi_{ij}} \tag{16}$$

$$F_3(u_i) = \left(1 - \frac{u_i}{r_i}\right)^{k\sin\psi_{ij}} \tag{17}$$

The displacement at the inner boundary of the shell ij can be determined through (14) from the strains in the previous element, the displacement u_j at the outer boundary of ij and the radii r_i and r_j. However, the dilatancy angle ψ_{ij}, which also appears in (14), should reflect the average stress conditions within the element ij, and thus iterations are required with the stresses to obtain the displacement and stress field in the plastic zone. This is described in the next section.

Numerical Implementation

The numerical procedure for cavity pressure determination is based on a recursive approach, moving from element to element, starting from the first element, whose outer boundary is the elastic-plastic interface. At the elastic-plastic interface, the radial and tangential normal stress σ_R and σ_T, the displacement u_R, and the radial, hoop and volumetric strains are all known (Salgado et al. 1997a). Once these variables are all determined for the inner boundary of the first element, which coincides with the outer boundary of the second element, then calculations can be made for the second element. For limit pressure determination, these recursive computations continue until the

calculated displacement at the inner boundary of some element becomes equal to the radius of that boundary. This implies cavity creation (i.e., expansion from zero initial radius), which in turn implies that the limit pressure has been reached.

At the elastic-plastic interface, the stress and strain tensor components are given by:

$$\sigma_R = p_0 \frac{(k+1)N_p}{N_p + k} \tag{18}$$

$$\sigma_T = \frac{\sigma_R}{N_p} \tag{19}$$

$$\varepsilon_\theta(r=R) = -\varepsilon_T \tag{20}$$

$$\varepsilon_T = \frac{N_p - 1}{N_p + k} \frac{p_0}{2G} \tag{21}$$

$$\varepsilon_r(r=R) = \varepsilon_R = k\,\varepsilon_T \tag{22}$$

In (18) though (22), N_p is the peak flow number, calculated from the peak friction angle through

$$N_p = \frac{1+\sin\phi_p}{1-\sin\phi_p} \tag{23}$$

where ϕ_p is obtained from either (5) or (7) with p_{ij} computed from σ_R and σ_T. Notice that an iteration is required to obtain ϕ_p and N_p. The shear modulus G is some fraction g_r of the small-strain shear modulus G_0:

$$G = g_r\, G_0 \tag{24}$$

where G_0 is usually expressed as a function of mean effective stress and void ratio through the empirical equation of Hardin and Black (1968):

$$\frac{G_0}{p_A} = C_g \frac{(e_g - e)^2}{1+e} \left(\frac{\sigma_m}{p_A} \right)^{n_g} \tag{25}$$

Progress from the elastic-plastic interface inward is made as follows:

1) Assume suitable values for ψ_{ij} and N_{ij};
2) Solve (14) for u_i; this is done generally using the Newton-Raphson algorithm, except for the element adjacent to the cavity in limit pressure computations, where the bisection method is used instead;
3) Calculate the inner radial normal stress σ_{ri} from (3) and the tangential normal stress by dividing σ_{ri} by N_{ij};
4) Using the Davis (1969) approach for accounting for the stress component in the zero strin direction, calculate p_{ij} from

$$p_{ij} = \frac{1}{3}[1+(2-k)\mu_{ij}] \left(1 + \frac{k}{N_{ij}} \right) \bar{\sigma}_r \tag{26}$$

where $\bar{\sigma}_r$ = average of σ_{ri} and σ_{rj} and, for k = 1,

$$\mu_{ij} = \frac{1}{2}(1 + \sin\phi_{ij} \sin\psi_{ij}) \tag{27}$$

5) Calculate the strains from r_i, r_j, u_i and u_j; from the volumetric strain, calculate a new void ratio and relative density;
6) Calculate a new ϕ_{ij} from either (5) or (7), depending on the model that is being used, and then N_{ij} and ψ_{ij};
7) Compare N_{ij} computed in step 6 with the one assumed in step 1; if the difference is not satisfactorily small, assume new values of N_{ij} and ψ_{ij} and restart from step 2.

The values of ψ_{ij}, ϕ_{ij} and N_{ij} are initially assumed to be the same as that of the previous element (or the peak values in the case of computations for the first element); it may be that this assumed value will not allow a solution to equation (14), in which case it needs to be decreased by a small amount. Once convergence for each element is

achieved, the value of the calculated displacement u_i is compared with the radius r_i. Calculations are continued for a new element if $r_i > u_i$. If $u_i = r_i$, the cavity wall has been reached and the limit pressure $p_L = \sigma_{ri}$. The thickness $r_j - r_i$ of all elements is the same, except for the very last element, which is allowed to have a different size in order to satisfy the limit condition $u_i = r_i$ more accurately. So long as a sufficiently small value of r_i-r_j is selected, convergence is always achieved. It has been found that subdivision of the plastic zone in 500 to 2000 elements, depending on the initial density and stress level, is sufficient for convergence.

4. Penetration Resistance Analysis

The penetration resistance q_c in sand may be calculated from p_L. Although a rigorous analysis that incorporates all the main features of sand mechanical behavior (e.g., critical state behavior, a dilatancy angle dependent upon density and stress, etc.) would be very difficult, an analysis with sufficient accuracy can be obtained if a few simplifying assumptions are made. Figure 2 shows a plane-strain, kinematically admissible slip mechanism that can be used to develop a suitable analysis. The cone surface is represented as a slip surface with interface friction angle δ_c. The semi-apex angle of the cone is θ_c. The mechanism can be viewed as a transition zone between the cone and the zone where the major principal effective stress is horizontal and associated with the expansion of a cylindrical cavity. The transition zone is composed of an infinite number of log-spiral slip surfaces, each represented by an equation with the form:

$$s = s_0 \exp (\Delta\lambda \tan\psi_T) \qquad (28)$$

where s = log-spiral radius measured from point B (the edge of the cone) where the cone surface meets with the cylindrical shaft of the penetrometer; s_0 = log-spiral radius BC; $\Delta\lambda$ = angle between log-spiral radius s at which principal stress becomes horizontal and s_0 =

BC; ψ_T = operative dilatancy angle for the transition zone. The initial point of the log-spiral, lying on the cone surface, has radius r_0, measured from the axis of the cone; the end point, lying on the line where the major principal stress turns horizontal, has radius r given by

$$r = a\,(1+C_\lambda) - r_0\,C_\lambda \tag{29}$$

where

$$C_\lambda = \begin{cases} \dfrac{\sin(\Delta\lambda - \theta_c)}{\sin\theta_c}\exp(\Delta\lambda\tan\psi_T) & \text{if } \phi_T \geq \phi_c \\ \dfrac{\sin(\Delta\lambda - \theta_c)}{\sin\theta_c} & \text{if } \phi_T < \phi_c \end{cases} \tag{30}$$

and

$$\Delta\lambda = \frac{\pi}{4} + \frac{\delta_c}{2} + \theta_c \tag{31}$$

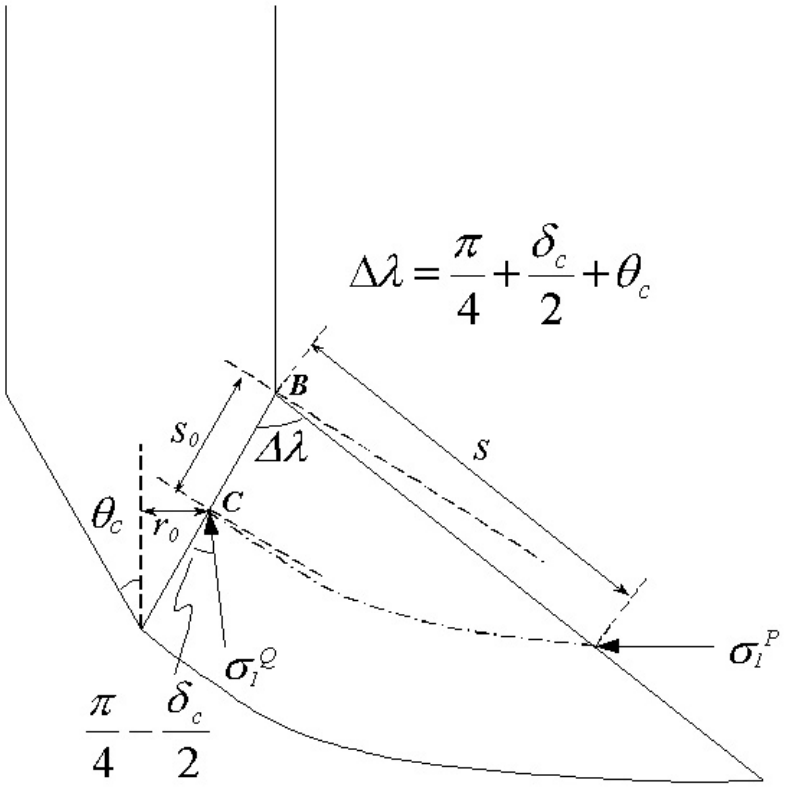

Figure 2 Slip mechanism for cone penetration.

Following the stress rotation analysis of Bolton (1982), the major principal stresses, separated by the transition zone with angle $\Delta\lambda$, are related through

$$\sigma'_1{}^Q = \sigma'_1{}^P \exp(2\,\Delta\lambda \tan\phi_T) \qquad (32)$$

where:

$\phi_T = \phi_c + 0.8\psi_T$ = transition zone friction angle;

$\sigma'_1{}^Q$ = major principal effective stress acting on the cone surface at the initial point of a given logspiral;

$\sigma'_1{}^P$ = major principal effective stress acting in the horizontal direction at the end point of the same logspiral (which is also the radial stress due to cavity expansion acting at the end of the log spiral), given by

$$\sigma'_1{}^{P} = p_L \left(1 + C_\lambda - C_\lambda \frac{r_0}{r_c}\right)^{\eta-1} \tag{33}$$

where

$$\eta = 1 - \frac{N_T - 1}{N_T} \tag{34}$$

$r_c = 0.5\ dc$ = cone radius

N_T = transition zone flow number, computed from the friction angle ϕ_T operative within the stress rotation zone.

The friction angle ϕ_T depends on q_c, which creates high confining stresses in the zone around the cone. The high confining stresses inhibit dilatancy and keep ϕ_T close in value to ϕ_c. Since q_c depends on ϕ_T, and ϕ_T depends on q_c through the confining stresses that q_c creates, the calculation of q_c is done iteratively.

Using (32),

$$\sigma'_1{}^{Q} = p_L \exp(2\Delta\lambda \tan\phi_T)\left(1 + C_\lambda - C_\lambda \frac{r_0}{r_c}\right)^{\eta-1} \tag{35}$$

The associated minor principal effective stress is given by

$$\sigma'_3{}^{Q} = \frac{\sigma'_1{}^{Q}}{N_c} \tag{36}$$

where the critical state flow number N_c is used because of the proximity to the cone surface, where the sand deformation is large and the critical state condition has been reached. Knowing the values of $\sigma'_1{}^{Q}$ and $\sigma'_3{}^{Q}$ at each point of the cone surface, it is possible, through integration over the area of the cone surface, to obtain the total vertical

force opposing penetration. Dividing the resulting vertical force by the projected cross-sectional area of the cone gives the cone resistance q_c:

$$q_c = 2\, f_v\, p_L \exp(2\Delta\lambda \tan\phi_T)\, \frac{(1+C_\lambda)^{\eta+1} - C_\lambda(\eta+1) - 1}{C_\lambda{}^2\eta(\eta+1)} \tag{37}$$

with:

$$f_v = \frac{1}{2}\left[\left(1+\frac{1}{N_c}\right) + \left(1-\frac{1}{N_c}\right)\left(\cos\delta_c \cot\theta_c - \sin\delta_c\right)\right] \tag{38}$$

where δ_c = steel-sand interface critical state friction angle and θ_c = cone semi-apex angle.

The starting point for finding the average mean effective stress in the transition zone, required for the calculation of ϕ_T, is to realize that q_c is the average vertical stress acting on the face of the cone. Working back from that, we find that the average radial stress acting on the cone face is given by

$$\bar{\sigma}'_r = 2\, p_L\, \frac{(1+C_\lambda)^{\eta+1} - C_\lambda(\eta+1) - 1}{C_\lambda{}^2\eta(\eta+1)} \tag{39}$$

and the associated mean effective stress can be written as:

$$\bar{p}_0 = \frac{1}{2}\left(1+\frac{1}{N_T}\right)\bar{\sigma}_r \tag{40}$$

Consider the slip line starting at the point on the cone surface where $\sigma'_v = q_c$ (which we may choose to call the "average" slip line). The mean effective stress varies along this slip line following:

$$\bar{p} = \bar{p}_0 \exp\left[2(\Delta\lambda - \xi)\tan\phi_T\right] \tag{41}$$

where ξ = angle ranging from 0 to $\Delta\lambda$ between an arbitrary log-spiral radius s and s_0 = BC.

Taking the average of $\bar{p}$ over the slip line:

$$\bar{p}_T = \begin{cases} \dfrac{\bar{p}_0}{2\tan\phi_T \cot\psi_T} \dfrac{\exp(2\Delta\lambda\tan\phi_T) - \exp(\Delta\lambda\tan\psi_T)}{\exp(\Delta\lambda\tan\psi_T) - 1} & \text{if } \phi_T \geq \phi_c \\ \bar{p}_T = \bar{p}_0 \dfrac{\exp(2\Delta\lambda\tan\phi_T) - 1}{2\Delta\lambda\tan\phi_T} & \text{if } \phi_T < \phi_c \end{cases} \tag{42}$$

Computation of q_c from p_L is done iteratively as follows:

1) assume value for ϕ_T (and thus ψ_T, N_T);
2) compute η, $\Delta\lambda$, C_λ; using eqs. (34), (31) and (30), respectively;
3) compute ϕ_T using the Bolton relationship (eq. (7)) with $p_{ij} = \bar{p}_T$;
4) iterate until convergence of assumed and calculated values of ϕ_T is reached;
5) compute q_c using (37) and (38).

There is no single value of friction angle in the immediate neighborhood of the cone, as the stress and strain fields are complex and change sharply. Along the cone surface and the penetrometer shaft, where shear strains are quite large, ϕ should be very approximately equal to ϕ_c both for contractive and dilative sands. Accordingly, the interface friction angle is taken as $\delta_c = 0.5\phi_c$ for the smooth steel of which cone penetrometers are made. However, near the cone surface but slightly away from the steel-

soil interface, stresses are very high and the sand is likely to undergo some crushing, which is difficult to model. According to Bolton (1986), it may be necessary to allow ϕ to be less than ϕ_c, as very contractive sands would require such large strains to develop ϕ_c that the operative, mobilized friction angle would be less than ϕ_c under most conditions of practical interest. So, for contractive sands (primarily sands with very low relative density), the computed transition zone friction angle is at most equal to ϕ_c, such that $\phi_T \leq \phi_c$. For dilative sands, where the high relative densitites and low to moderate initial confining stresses are likely to lead to ϕ values greater than ϕ_c even within the transition zone, we allow $\phi_T \geq \phi_c$. We distinguish dilative from contractive sands as follows: if the peak friction angle ϕ_p calculated for the elastic-plastic interface is less than ϕ_c, the sand is a contractive sand; it is dilative otherwise.

5. Instructions

Input File Preparation

Prepare three input files. You can call them anything you wish, but save the names as you will need to enter them when prompted by the program. We will call them the INPUT, SMODEL and COMPUT files. The INPUT file contains parameters associated with the soil state(s) for which you wish calculations done, plus the information of whether you wish cylindrical (K = 1) or spherical (K=2) cavity pressures to be calculated. Remember: for cone resistance to be computed, you must select cylindrical (K=1). The SMODEL file contains information concerning the soil and the cone penetrometer. The COMPUT file contains initial parameters for the computations to be carried out.

EACH LINE OF THE **COMPUT** FILE MUST CONTAIN THE FOLLOWING:

MODEL = 'BOLTON' , 'STATEP' OR 'LAGIOIA'

R = PLASTIC RADIUS (suggested value = 100)

DIVR0 = INITIAL ELEMENT THICKNESS DIVISOR (suggested value = 400; el th = R/DIVR)

PA = REFERENCE STRESS = 100 kPa = 0.1 MPa = 0.1 kgf/cm2 = 0.1 tsf

THETAC = SEMIAPEX ANGLE OF CONE PENETROMETER (standard value = 30°)

DELRAT = RATIO OF LARGE-STRAIN STEEL-SOIL INTERFACE FRICTION ANGLE TO THE LARGE-STRAIN (CRITICAL STATE) FRICTION ANGLE OF THE SAND (suggested value = 0.5)

Example:

'BOLTON',100.D+00,600.D+00,100.D+00,30.0D+00,0.5D+00

EACH LINE OF THE **INPUT** FILE MUST CONTAIN THE FOLLOWING:

PROJECT = PROJECT ID (UP TO 20 CHARACTERS);

ADDITIONAL COMMENT (up to 20 characters)

K = 1 (FOR CYLINDRICAL) or K = 2 (FOR SPHERICAL CAVITY EXPANSION);

DR = RELATIVE DENSITY;

SIGV = VERTICAL EFFECTIVE STRESS;

SIGH = HORIZONTAL EFFECTIVE STRESS;

Example:

'20%,' 12.5 kPa',1,20.D+00,31.25D+00,12.5D+00

'20%','25 kPa',1,20.D+00,62.5D+00,25.D+00

'20%','50 kPa',1,20.D+00,125.D+00,50.D+00

'20%','75 kPa',1,20.D+00,187.5D+00,75.D+00

'20%,' 100 kPa',1,20.D+00,250.D+00,100.D+00

'20%,' 150 kPa',1,20.D+00,375.D+00,150.D+00

'20%,' 200 kPa',1,20.D+00,500.D+00,200.D+00

'20%,' 250 kPa',1,20.D+00,625.D+00,250.D+00

'20%,' 300 kPa',1,20.D+00,750.D+00,300.D+00

EACH LINE OF THE **SMODEL** FILE MUST CONTAIN THE FOLLOWING:

FOR THE BOLTON MODEL,

PHICR = CRITICAL STATE FRICTION ANGLE

Q,RQ = TWO PARAMETERS OF BOLTON (1986) FRICTION ANGLE CORRELATION

EMAX,EMIN = MAXIMUM AND MINIMUM VOID RATIOS

CG,EG,NG = PARAMETERS IN SMALL-STRAIN SHEAR MODULUS GMAX CORRELATION

GRAT = RATIO OF G TO GMAX FOR FREE-FIELD CONDITIONS (recommended value = 0.68)

NI = POISSON'S RATIO;

FOR THE STATE PARAMETER MODEL,

PHICR = CRITICAL STATE FRICTION ANGLE

LAMBDAC,GAMMA= PARAMETERS IN STATE PARAMETER DEFINITION

A= PARAMETER TO CALCULATE PHI FROM STATE PARAMETER

EMAX,EMIN = MAXIMUM AND MINIMUM VOID RATIOS

CG,EG,NG = PARAMETERS IN SMALL-STRAIN SHEAR MODULUS GMAX CORRELATION

GRAT = RATIO OF G TO GMAX FOR FREE-FIELD CONDITIONS

NI = POISSON'S RATIO

FOR THE LAGIOIA MODEL (still under implementation)

PHICR = CRITICAL STATE FRICTION ANGLE

ALPHA, MU = PARAMETERS IN LAGIOIA (1996) MODEL

EMAX,EMIN = MAXIMUM AND MINIMUM VOID RATIOS

CG,EG,NG = PARAMETERS IN SMALL-STRAIN SHEAR MODULUS GMAX CORRELATION

GRAT = RATIO OF G TO GMAX FOR FREE-FIELD CONDITIONS

Examples:

Hokksund Sand: Bolton Model

36.0+00,10.D+00,1.0D+00,0.87D+00,0.55D+00,942.D+00,1.96D+00,0.46D+00,0.68D+00,0.15D+00

Hokksund Sand: State Parameter Model

36.0+00,0.0234D+00,1.826D+00,0.80D+00,0.87D+00,0.55D+00,942.D+00,1.96D+00,0.46D+00,0.68D+00,0.15D+00

Ticino Sand: Bolton Model

34.8+00,10.D+00,1.0D+00,0.93D+00,0.57D+00,647.D+00,2.27D+00,0.43D+00,0.68D+00,0.15D+00

Ticino Sand: State Parameter Model

34.8+00,0.0243D+00,1.874D+00,0.60D+00,0.93D+00,0.57D+00,647.D+00,2.27D+00,0.43D+00,0.68D+00,0.15D+00

A Note on the Use of the Different Models

The Bolton model has an implicit critical state line that curves sharply at large mean effective stress values. This is in sharp contrast with the state parameter model, which assumes a straight critical state line. Accordingly, results will per force be different for the two models.

Running the Program

Run the program by typing CONPOINT in the prompt. The program will ask you for the names of the input files you prepared, as well as for the names you wish to give to two of the output files: the text output file and the excel summary file. After you have entered these names, calculations start.

Progress of calculations will appear on the screen. The program will start calculations with the number of elements set in the comput.i file. If it finds the initial thickness of the elements does not produce results, it will adjust element thickness (and the number of elements) for the initial run. After the first run is complete, it will then increase the number of elements by 50% to obtain an additional result. If the results are close to within a pre-set tolerance, it will move on to the next data line; if not, it will again increase the number of elements and repeat the calculations. It is possible that no convergence will take place for a given data line for initial number of elements you selected in the input file COMPUT. In this case, the program increases the initial number of elements and restarts calculations until an error less than 1.5% is obtained on the limit pressure. You can see this by looking at the PL error in the EXCEL summary output file. This is the relative error in the limit pressure calculated for the same data line for the last two runs (the last run has 50% more elements than the one preceding it).

You will obtain four output files. Ignore cc.xls and ccs.xls. The three to focus on are the two files you named (the text and excel output files) and plzone.xls. The excel file contains the summary results for each line of the input file. The plzone.xls file contains the values of such quantities as friction and dilatancy angles for each soil element within the plastic zone. It allows observation of the evolution of soil state and related quantities as a function of distance from the cavity and elastic-plastic interface. It is a large file that is written over every time the program is run, unless you save it for later examination.

6. Sample Calculations

Cylindrical Expansion in Contractive Ticino Sand

Input file for D_R = 20% and several initial effective stress states:

'EXAMPLE 1','20% 12.5 kPa',1,20.D+00,31.25D+00,12.5D+00

'EXAMPLE 1','20% 25 kPa',1,20.D+00,62.5D+00,25.D+00

'EXAMPLE 1','20% 50 kPa',1,20.D+00,125.D+00,50.D+00

'EXAMPLE 1','20% 75 kPa',1,20.D+00,187.5D+00,75.D+00

'EXAMPLE 1','20% 100 kPa',1,20.D+00,250.D+00,100.D+00

'EXAMPLE 1','20% 150 kPa',1,20.D+00,375.D+00,150.D+00

'EXAMPLE 1','20% 200 kPa',1,20.D+00,500.D+00,200.D+00

'EXAMPLE 1','20% 250 kPa',1,20.D+00,625.D+00,250.D+00

'EXAMPLE 1','20% 300 kPa',1,20.D+00,750.D+00,300.D+00

The appendix contains the summary excel files obtained for the Bolton model for this input file. Figure 3 shows in e-log p space the evolution of soil state with cavity expansion for several of the input file data lines. Note that at the cavity wall, the soil state falls on the critical state line, as expected. The critical state line implicit in the Bolton model is curved as seen in the figure. For similar plots for the state parameter model, please refer to the paper by Salgado and Randolph (2001) in the International Journal of Geomechanics.

Figure 3 Void ratio vs. pressure for the cavity expansion processes of the sample input files.

Cylindrical Expansion in Dilatant Ticino Sand

Input file for D_R = 80% and several initial effective stress states:

'EXAMPLE 2','80% 12.5 kPa',1,80.D+00,31.25D+00,12.5D+00

'EXAMPLE 2','80% 25 kPa',1,80.D+00,62.5D+00,25.D+00

'EXAMPLE 2','80% 50 kPa',1,80.D+00,125.D+00,50.D+00

'EXAMPLE 2','80% 75 kPa',1,80.D+00,187.5D+00,75.D+00

'EXAMPLE 2','80% 100 kPa',1,80.D+00,250.D+00,100.D+00

'EXAMPLE 2','80% 150 kPa',1,80.D+00,375.D+00,150.D+00

'EXAMPLE 2','80% 200 kPa',1,80.D+00,500.D+00,200.D+00

'EXAMPLE 2','80% 250 kPa',1,80.D+00,625.D+00,250.D+00

'EXAMPLE 2','80% 300 kPa',1,80.D+00,750.D+00,300.D+00

Note that we have used the same K_0 for both 20 and 80% relative density. Conceptually, it would be better to use a slightly lower K_0 for the dense sand.

The appendix contains the summary excel files obtained for the Bolton model for this input file. Figure 3 shows in e-log p space the evolution of soil state with cavity expansion for several of the input file data lines. Note that at the cavity wall, the soil state falls on the critical state line, as expected. The critical state line implicit in the Bolton model is curved as seen in the figure. For similar plots for the state parameter model, please refer to the paper by Salgado and Randolph (2001).

References

Been, K. and Jefferies, M.G. (1985). "A State Parameter for Sands." Geotechnique 35(2), 99-112.

Bigoni, D. and Laudiero, F. (1989). "The Quasi-Static Finite Cavity Expansion in a Non-Standard Elasto-Plastic Medium", Int. J. Mech. Sci., Vol. 31, No. 11/12, pp. 825-837.

Bolton, M. D. (1986). "The Strength and Dilatancy of Sands." Geotechnique 36(1), 65-78.

Carter, J. P., Randolph, M. F. and Wroth, C. P. (1979). "Stress and Pore Pressure Changes in Clay During and After the Expansion of a Cylindrical Cavity." International Journal for Numerical and Analytical Methods in Geomechanics 3, 305-322.

Carter, J. P., Booker, J. R. and Yeung, S. K. (1986), "Cavity Expansion in Cohesive Frictional Soils", Geotechnique 36, No. 3, pp 349-358.

Chadwick, P. (1959). "The Quasi-Static Expansion of a Spherical Cavity in Metals and Ideal Soils. Part I" Quart. J. Mech. Appl. Math. 12, 52-71.

Collins, I.F., Pender, M.J. and Yan, W. (1992). "Cavity Expansion in Sands under Drained Loading Conditions." International Journal for Numerical and Analytical Methods in Geomechanics 16, 3-23.

Davis, E. H. (1969). "Theories of Plasticity and the Failure of Soil Masses." Soil Mechanics Selected Topics, Chap. 6, Lee, I. K., ed., London, Butterworths, 341-380.

Davis, R. O., Scott, R. F. and Mullenger, G. (1984). "Rapid Expansion of a Cylindrical Cavity in a Rate-Type Soil." International Journal for Numerical and Analytical Methods in Geomechanics, Vol. 8, pp. 125-140.

Fahey, M. (1986). "Expansion of a Thick Cylinder of Sand: a Laboratory Simulation of the Pressuremeter Test." Geotechnique 36(3), 397-424.

Hardin, B. and Black, W. (1968). "Shear Modulus and Damping in Soils." J. Soil Mechs. Found. Div., 94(2), 353-369.

Ladanyi, B. (1963). "Expansion of a Cavity in a Saturated Clay Medium." Journal of the Soil Mechanics and Foundations Division, Proceedings of the American Society of Civil Engineers, Vol. 89, No. SM4, July, pp. 127-161.

Manassero, M. (1989). "Stress-Strain Relationships from Drained Self-Boring Pressuremeter Tests in Sand." Geotechnique 39(2), 293-308.

Palmer, A.C. (1972). "Undrained Plane-Strain Expansion of a Cylindrical Cavity in Clays." Geotechnique 22(3), 451-457.

Randolph, M.F. and Wroth, C.P. (1979). "An Analytical Solution for the Consolidation Around a Driven Pile." International Journal for Numerical and Analytical Methods in Geomechanics, 3, 217-229.

Randolph, M.F., Carter, J.P. and Wroth, C.P. (1979). "Driven Piles in Clay – The Effects of Installation and Subsequent Consolidation." Geotechnique 29(4), 361-393.

Rowe, P. (1962),"The Stress-Dilatancy Relation for Static Equilibrium of an Assembly of particles in contact", Proc. R. Soc., Series A, Vol. 269, 500.

Salgado, R. and Mitchell, J.K (2002). "Computation of Cone Resistance in Sands." Working paper (find it at www.ecn.purdue.edu/~rodrigo/)

Salgado, R. and Randolph, M.F. (2001). "Analysis of Cavity Expansion in Sand", International Journal of Geomechanics, 1(2), 175-192.

Salgado, R., Mitchell, J. K., and Jamiolkowski, M. B. (1997a). "Cavity Expansion and Penetration Resistance in Sands." Journal of Geotechnical and Geoenvironmental Engineering, ASCE, 123(4), 344-354.

Salgado, R., Boulanger, R. and Mitchell, J.K. (1997b). "Lateral Stress Effects on CPT Liquefaction Resistance Correlations." Journal of Geotechnical and Geoenvironmental Engineering, ASCE, 123(8), 726-735.

Salgado, R., Mitchell, J. K., and Jamiolkowski, M. B. (1998). "Chamber Size Effects on Penetration Resistance Measured in Calibration Chambers." Journal of Geotechnical and Geoenvironmental Engineering, ASCE, 124(9), 878-888.

Salgado, R., Bandini, P. and Karim, A. (2000). "Shear Strength and Stiffness of Silty Sands." Journal of Geotechnical and Geoenvironmental Engineering, ASCE, 126(5), 451-462.

Vésic, A. S. (1972), "Expansion of Cavities in Infinite Soil Mass", J. Soil Mech. Found. Div., ASCE, March.

Vésic A. S. (1977), "Design of Pile Foundations", Synthesis of Highway Practice No. 42, Nat. Coop. Highway Research Prog., Transportation Research Board, Washington, D.C., 68 pages.

Yu, H. S. and Houlsby, G. T. (1991), "Finite Cavity Expansion in Dilatant Soils: Loading Analysis", Geotechnique 41(2), 173-183.

Feedback

Feedback is appreciated as we attempt to perfect this program and make it more user-friendly. Please write to

Prof. Rodrigo Salgado
School of Civil Engineering
Purdue University
West Lafayette IN 47907-1284
(765)496-1364 (FAX)
rodrigo@ecn.purdue.edu
http://www.ecn.purdue.edu/~rodrigo/